

# Propagation of very high energy gamma-rays inside massive binaries LS 5039 and LSI + 61° 303

W. Bednarek<sup>?</sup>

Department of Experimental Physics, University of Lodz, ul. Pomorska 149/153, 90-236 Lodz, Poland

Accepted . Received ; in original form

## ABSTRACT

Two massive binary systems of the microquasar type, LS 5039 and LSI + 61° 303, have been suggested as possible counterparts of EGRET sources. LS 5039 has been also recently detected in TeV gamma-rays. Since the massive stars in these binary systems are very luminous, it is expected that high energy gamma-rays, if injected relatively close to the massive stars, should be strongly absorbed, initiating inverse Compton electron cascades in the anisotropic radiation from stellar surfaces. We investigate influence of the propagation effects on the spectral and angular features of the gamma-ray spectra emerging from these two binary systems by applying the Monte Carlo method. Two different hypotheses are considered: isotropic injection of primary gamma-rays with the power law spectrum due to e.g. interaction of hadrons with the matter of the wind, and the isotropic injection of electrons, e.g. accelerated in the jet, which Comptonize the radiation from the massive star. It is concluded that propagation effects of gamma-rays can be responsible for the spectral features observed from LS 5039 (e.g. the shape of the spectrum in the GeV and TeV energy ranges and their relative luminosities). The cascade processes occurring inside these binary systems significantly reduce the gamma-ray opacity obtained in other works by simple calculations of the escape of gamma-rays from the radiation fields of the massive stars. Both systems provide very similar conditions for the TeV gamma-ray production at the periastron passage. Any TeV gamma-ray flux at the apastron passage in LSI + 61° 303 will be relatively stronger with respect to its GeV flux than in LS 5039. If gamma-rays are produced inside these binaries not far from the massive stars, i.e. within a few stellar radii, then clear anticorrelation between the GeV and TeV emission should be observed, provided that primary gamma-rays at GeV and TeV energies are produced in the same process by the same population of relativistic particles. These gamma-ray propagation features can be tested in the near future by the multi-wavelength campaigns engaging the AGILE and GLAST telescopes (> 30 MeV) and the Cherenkov telescopes (> 100 GeV, e.g. MAGIC, HESS, VERITAS and CANGAROO).

**Key words:** binaries: close – stars: LS 5039, LSI + 61° 303 – radiation mechanisms: non-thermal – gamma-rays:

## 1 INTRODUCTION

Massive binary systems provide very promising conditions for acceleration of particles to relativistic energies and also well defined conditions for their possible interaction. Therefore, they have been considered for a long time as possible sources of high energy gamma-rays and neutrinos in which acceleration processes can be tested. In fact, some GeV gamma-ray sources observed by EGRET detector (> 100 MeV) have been proposed to be related to well known massive bina-

ries in which non-thermal processes were evident at lower energies, e.g. LSI + 61° 303 (2EG J0241+ 6119; Thompson et al. 1995), Cen X-3 (Vestrand, Sreekumar & Mori 1997), Cyg X-3 (2EG J2033-4112; Mori et al. 1997), and LS 5039 (3EG J1824-1514; Paredes et al. 2000). Early searches of the TeV gamma-ray signals from massive binaries have not been very convincing, with the exception of Cen X-3 binary system (containing slowly rotating neutron star) which has been reported as TeV gamma-ray source by the Durham group (Chadwick et al. 1998, 1999, Atoyan et al. 2002). The turning-point came recently with the observations of TeV gamma-ray signals from two massive binaries: PSR B1259-63/SS 2883, contain-

<sup>?</sup> E-mail: bednar@zwe4.cuni.lodz.pl

ing a radio pulsar with the period of 47.8 ms (Aharonian et al. 2005a), and LS 5039, so called microquasar possibly containing a solar mass black hole (Aharonian et al. 2005b).

The  $\gamma$ -ray emission from massive binaries is usually interpreted in terms of the inverse Compton scattering (ICS) model in which thermal radiation coming from the stellar surface is scattered by electrons accelerated in the pulsar wind shock (e.g. Maraschi & Treves 1981) or by electrons moving highly anisotropically in the form of beams or jets (e.g. Bednarek et al. 1990). The binary systems which are considered as an example in this paper, LS 5039 and LSI + 61° 303, have been recently discussed in terms of the microquasar IC model by Bosch-Ramón & Paredes (2004a,b) and Paredes, Bosch-Ramón & Romero (2005). Primary  $\gamma$ -rays might be also produced in the microquasar scenario of the binary system as a result of the interaction of hadrons, accelerated in the jet, with the matter of the stellar wind (Romero, Christiansen & Orellana 2005). For review of the  $\gamma$ -ray production in microquasars see e.g. Romero (2004) or Paredes (2005).

The problem of importance of the propagation of TeV  $\gamma$ -rays inside compact massive binary systems appeared at the early 80's after first reports on possible observation of such  $\gamma$ -rays (see e.g. Weekes 1988). The optical depths for  $\gamma$ -rays in the radiation field of the accretion disk around the compact object inside the binary system have been calculated by e.g. Carramiñana 1992 and Bednarek (1993) and in the radiation field of the massive star by e.g. Protheroe & Stanev 1987 and Moskalenko, Karakula & Tkaczyk 1993). In the case of very compact binaries, the TeV  $\gamma$ -rays injected close to the surface of the massive star initiate the Inverse Compton  $e^+e^-$  pair cascade. The conditions for which the cascade processes should become important have been considered by Bednarek (1997, Sect. 2) and Dubus (2005, Sect. 6). In general, the product of the massive star luminosity and the square of its surface temperature should be much greater than  $10^{45} \text{ erg s}^{-1} \text{ K}^2$  (see Eq. 1 and Fig. 3 in Bednarek 1997). The  $\gamma$ -ray spectra which emerge toward the observer from such compact binary systems strongly depend on the phase of the injection place of the primary relativistic particles in respect to the observer. At some phases significant TeV  $\gamma$ -ray fluxes are expected but at others only photons with energies extending to a few tens GeV are able to escape (see detailed calculations of such anisotropic cascades and their application to specific sources, e.g. Cen X-3 and Cyg X-3, in Bednarek 1997 (B97), Bednarek 2000 (B00), and Sierpowska & Bednarek 2005 (SB05)). Recently, optical depths of TeV  $\gamma$ -rays have been calculated for other TeV  $\gamma$ -ray sources, LS 5039, PSR 1259-63 and LSI + 61° 303, without taking into considerations the effects of the IC  $e^+e^-$  pair cascading (Böttcher & Dörmmer 2005 and Dubus 2005).

Note that only calculations by Bednarek and collaborations (B97, B00, SB05) and Dubus (2005) take into account dimensions of the massive star. Therefore, they can be applied to very compact binaries in which injection distance of the TeV  $\gamma$ -rays from the center of massive stars is comparable to their radii, e.g. at the periastron passage of the compact objects in LS 5039 and LSI + 61° 303, or in the case of propagation of  $\gamma$ -rays injected at larger distances but passing close to the surface of the massive stars. The comparison of the exact calculations with the approximate ones,

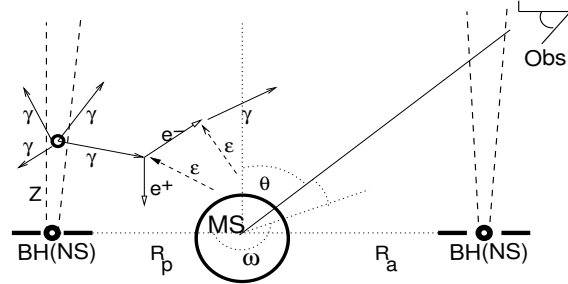


Figure 1. Schematic picture of a compact binary system composed of a massive star and a compact object (a black hole or a neutron star) on an orbit around the massive OB star. The observer is located at the inclination angle  $\theta$  and the azimuthal angle  $\phi$ . The matter accreting onto a compact object from the massive star creates an accretion disk. Particles (electrons or protons) are accelerated inside the jet launched from the inner part of an accretion disk. Primary electrons and/or  $\gamma$ -rays, injected at the distance  $z$  from the base of the jet, initiate an anisotropic inverse Compton  $e^+e^-$  pair cascade in the radiation field of the massive star. A part of the primary  $\gamma$ -rays and secondary cascade  $\gamma$ -rays escape from the binary system toward the observer.

which neglect dimensions of the massive stars, can be found in Dubus (2005).

In this paper we concentrate on details of the propagation of high energy  $\gamma$ -rays injected close to the surface of the massive star taking into account the effects of cascades initiated through the Inverse Compton and  $e^+e^-$  pair production processes. We calculate the  $\gamma$ -ray spectra emerging to the observer from such anisotropic cascades for two compact massive binaries LS 5039 (already reported in GeV and TeV  $\gamma$ -rays) and LSI + 61° 303 (reported only at GeV energies). Specific cases with the injection of primary  $\gamma$ -rays (e.g. by relativistic hadrons) or electrons (accelerated in the jet or the shock) with simple power law spectra and spectral indexes equal to 2 are considered in order to better understand the basic features of such anisotropic cascade processes.

## 2 THE MASSIVE BINARY SYSTEMS

Both binary systems considered in this paper belong to the class of the non-thermal radio high mass X-ray binaries showing evidences of collimated relativistic outflows. They are called microquasars due to their supposed similarities to quasars which show very narrow jets moving with relativistic speeds. In binary systems jets are launched from the inner parts of accretion disks around compact objects (a neutron stars or a solar mass black holes).

Here we consider a simple scenario in which jets are launched along the disk axis. The surface of the disk is in the plane of the binary system, i.e. the jet direction is perpendicular to the plane of the binary system. The schematic picture of such binary system is drawn in Fig. 1. Relativistic particles, injected in the jet at the distance  $z$  from its base, produce  $\gamma$ -rays. If the injection site of the  $\gamma$ -rays is relatively close to the massive star,  $\gamma$ -rays interact with the stellar radiation initiating the IC  $e^+e^-$  pair cascade. The efficiency of such cascades depend strongly on the parameters of the binary systems LS 5039 and LSI + 61° 303. These two binaries

differ in basic parameters, e.g. their orbital periods are equal to 3.9 days and 26.5 days. However both of them provide conditions in which cascading effects have to be taken into account when considering  $\gamma$ -ray production processes.

### 2.1 The binary system LS 5039

This binary system shows relativistic radio jets on milliarc-second scales, with the speed of  $v = 0.3c$  (Paredes et al. 2000). It has been also suggested to be a counterpart of the EGRET source 3EG J1824-1514 localized at  $0.5^\circ$  (Paredes et al. 2005). This source has relatively flat spectrum above 100 MeV, spectral index  $< 2$ , and the  $\gamma$ -ray luminosity  $4 \cdot 10^5 \text{ erg s}^{-1}$ . Moreover, the position of LS 5039 is consistent at the 3 $\sigma$  level with recently detected TeV source HESS J1826-148 (Aharonian et al. 2005). The spectrum above 250 GeV is also flat with the photon index  $2.12 \pm 0.15$ , although the luminosity is only  $10^3 \text{ erg s}^{-1}$ , about two orders of magnitude less than at GeV energies. Recent analysis of the TeV  $\gamma$ -ray light curve by Casares et al. (2005b), using new orbital parameters, show possible flux variations of a factor  $\sim 3$  with the maximum around the phase 0.9.

The basic parameters of the binary system LS 5039 has been recently reported by Casares et al. (2005b): the semi-major axis,  $a = 3.4r_*$ , ellipticity  $e = 0.35 \pm 0.04$ , the azimuthal angle of the observer in respect to the periastron passage,  $\phi = 225^\circ$ , radius of the massive star,  $r_* = 9.3^{+0.7}_{-0.6} R_\odot$ , and its surface temperature,  $T_s = 3.9 \cdot 10^4 \text{ K}$ . For these parameters the distance of the compact object from the massive star changes in the range:  $r_p = 2.2r_*$  at the periastron up to  $r_a = 4.5r_*$  at the apastron. The estimated inclination angle of the binary system toward the observer depends on the mass of the compact object. It is estimated on  $\phi = 24.9 \pm 2.8^\circ$  for the case of the black hole with the mass  $3.7M_\odot$  and on  $60^\circ$  for the neutron star (Casares et al. 2005b). We present the results of numerical calculations for both inclination angles in the case of LS 5039.

### 2.2 The binary system LSI + 61° 303

LSI + 61° 303 has been also observed as a non-spherical radio source, which structure was interpreted as due to relativistic radio jets, the speed of  $0.6c$ , with some hints of its precession (Massi et al. 2004). It has been pointed out (Gregory & Taylor 1978) that this source is connected with the COS B  $\gamma$ -ray source CG 135+01 (Hermesen et al. 1977). CG 135+01 has been also detected by EGRET ( $> 100 \text{ MeV}$ ); the source 2EG J0241+6119 has a hard spectrum with photon spectral index  $2.05 \pm 0.06$  (Knien et al. 1997), and by COMPTEL in the energy range  $0.75$  to  $30 \text{ MeV}$ , spectral index  $1.95^{+0.2}_{-0.3}$  (van Dijk et al. 1996). The analysis of different EGRET observations shows evidences of variability (Tavani et al. 1998, confirmed by Wallace et al. 2000) with probable modulation with the orbital period of LSI + 61° 303 and the maximum emission near the periastron passage (Massi 2004). The Whipple group (Hallet et al. 2003) puts an upper limit on the TeV flux from this source,  $10^{11} \text{ cm}^{-2} \text{ s}^{-1}$  above  $500 \text{ GeV}$  ( $< 1.3 \cdot 10^{12} \text{ erg s}^{-1}$ ), which is clearly below an extrapolation of the EGRET spectrum.

The basic parameters of the binary system LSI + 61°

303 has been recently reported by Casares et al. (2005a): the semi-major axis  $a = 5.3r_*$ , ellipticity  $e = 0.72$ , the inclination of the binary system toward the observer is not well constrained by the observations (Casares et al. 2005):  $25^\circ < i < 60^\circ$  for a neutron star and  $i < 25^\circ$  for a black hole. We apply the value of  $i = 30^\circ$ . The azimuthal angle of the observer in respect to the periastron passage is  $\phi = 70^\circ$ , radius of the massive star  $r_* = 13.4 R_\odot$ , and its surface temperature  $T_s = 2.8 \cdot 10^4 \text{ K}$ . For these parameters the distance of the compact object from the massive star changes in the range:  $r_p = 1.5r_*$  at the periastron up to  $r_a = 9.15r_*$  at the apastron. We apply these parameters in our further calculations.

## 3 OPTICAL DEPTHS FOR $\gamma$ -RAYS

The optical depths for  $\gamma$ -rays (for the process  $\gamma \rightarrow e^+e^-$ ) in the radiation field of the massive star, determined by the radius of the star and its surface temperature, are calculated in the general case, i.e. for an arbitrary place of injection of  $\gamma$ -ray photons with arbitrary energies and angles of propagation (see also B97, B00, SB05). This approach allows us to calculate the optical depths even for the primary  $\gamma$ -rays injected at the surface of the massive star. Therefore, it can be applied for studies of the cascade processes initiated by  $\gamma$ -ray photons since secondary  $\gamma$ -rays can appear, in principle, everywhere inside the binary system. In fact, the optical depths for the  $\gamma$ -rays propagating in the thermal radiation of these massive stars can be obtained by simple re-scaling of the earlier calculations for the massive star in Cen X-3 (shown e.g. in Bednarek 2000, Fig. 2), since they are proportional to the fourth power of the surface temperature and the square of the radius of the massive star. Also a shift in energy proportional to the surface temperature is necessary. Note, that in the case of cascade processes discussed in this paper, primary particles propagating at specific direction can contribute to the  $\gamma$ -ray spectra escaping at other directions. Therefore, for easier analysis of the obtained results, we show here the optical depths for  $\gamma$ -rays injected at the distance of the periastron and the apastron passages of the compact object around the massive stars in LS 5039 (Fig. 2a,b) and LSI + 61° 303 (Fig. 2c,d), as a function of the photon energy and their arbitrary injection angles,  $\theta$ , measured from direction defined by the centers of the companion stars, toward the massive star.

As expected, the optical depths strongly depend on the injection parameters (photon energy, angles of propagation) and the parameters of the massive star. The optical depths reaches the maximum corresponding to the peak in the black body spectrum of soft photons. The maximum optical depth shifts to larger photon energies with decreasing angle (provided that  $\theta$  is smaller than the angle  $\theta_*$ , intercepted by the massive star observed from the distance of the injection place). The optical depths are lower for  $\theta > \theta_*$ , since in this case  $\gamma$ -rays propagate only to the surface of the massive star (see full thick curves in Figs. 2a and c).  $\gamma$ -rays with energies  $> 1 \text{ TeV}$ , injected at the periastron distance in LS 5039,  $2.2r_*$ , are absorbed ( $\tau > 1$ ) for most of the propagation directions, except a small cone with the angular extend of  $\sim 40^\circ$ . At the apastron distance,  $4.5r_*$ , the escape cone increases to  $\sim 60^\circ$ . Only within such small

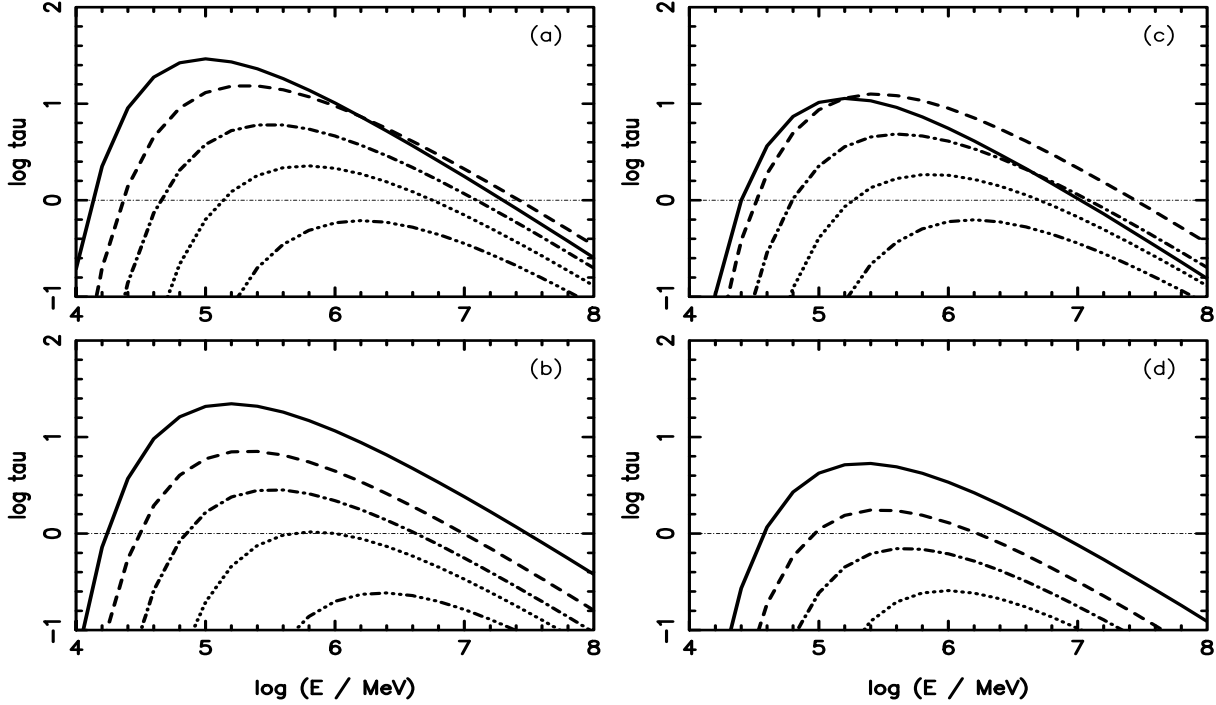


Figure 2. The optical depths for  $\gamma$ -rays (as a function of their energy) on  $e^+e^-$  pair production in collisions with stellar photons.  $\gamma$ -rays are injected at two distances from the massive star in LS 5039 ( $2.2r_2$  (a) and  $4.5r_2$  (b)) and in LSI + 61° 303 ( $1.5r_2$  (c) and  $9.15r_2$  (d)), corresponding to the periastron and the apastron passages, respectively. Specific curves show the optical depths for the injection angles of  $\gamma$ -rays measured from the direction defined by the centers of the stars:  $\theta = 150^\circ$  (full curve, direction toward the massive star),  $120^\circ$  (dashed),  $90^\circ$  (dotted),  $60^\circ$  (dot-dashed), and  $30^\circ$  (dot-dot-dot-dashed). The optical depths are calculated up to the infinity except two cases (marked by full curves in (a) and (c)) which are calculated to the surface of the massive star.

cones,  $\gamma$ -rays with  $\sim 1$  TeV energy have high chance to escape without absorption. The optical depth for  $\gamma$ -rays in LSI + 61° 303 are typically lower due to significantly lower surface temperature of the massive star. At the periastron distance,  $1.5r_2$ , the escape cone for  $\sim 1$  TeV  $\gamma$ -rays is also

$40^\circ$ , very similar to the periastron distance in LS 5039, due to the closer location of the injection place. However, at the apastron distance,  $9.15r_2$ , most of  $\sim 1$  TeV  $\gamma$ -rays escape from the binary system without absorption, except  $\gamma$ -rays moving toward the massive star within the cone with the angle  $\sim 80^\circ$ .

In LS 5039, the angles between the observer (at the inclination angle  $25^\circ$ ) and the direction defined by the stars are  $110^\circ$  for the periastron passage and  $70^\circ$  for the apastron passage. For such geometry, the optical depths towards the observer are larger than unity for  $\gamma$ -rays with energies in the range  $0.03 - 20$  TeV, for the periastron passage, and

$0.2 - 2$  TeV, for the apastron (see Fig. 2a,b). These calculations of the optical depths are generally consistent with that obtained by Dubus (2005).

In LSI + 61° 303, the observer is located at the angle of  $80^\circ$  at the periastron passage and at  $100^\circ$  at the apastron passage. In this case the optical depths are larger than unity for  $\gamma$ -rays with energies in the range  $0.1 - 10$  TeV for the periastron passage, but always lower than unity for the apastron, provided that they are injected toward the observer (see Fig. 2c,d).

#### 4 THE CASCADE $\gamma$ -RAY SPECTRA

Since the optical depths for high energy  $\gamma$ -rays in the radiation fields of the massive stars in binary systems LS 5039 and LSI + 61° 303 are large, the total  $\gamma$ -ray spectra, emerging from the binary systems toward the observer, are determined by the primary  $\gamma$ -ray spectra (if such are produced e.g. by hadrons accelerated in the jet) and by the  $\gamma$ -ray spectra produced in the IC  $e^+e^-$  pair cascades occurring in the radiation of the massive star. However, since the injection place of primary  $\gamma$ -rays or primary electrons is different than the center of the massive star (the source of isotropic soft radiation), the IC  $e^+e^-$  pair cascade occurs in fact in the anisotropic radiation field. IC  $e^+e^-$  pair cascades of such type have been already considered by us under two extreme assumptions. In the first approximation, local isotropization of the secondary cascade  $e^+e^-$  pairs by the random component of the magnetic field inside the stellar wind and the jet is assumed (see B97, B00). In the second approach, we follow the paths of secondary cascade  $e^+e^-$  pairs in the magnetic field which structure is described by a specific model (see SB05). In the present work we apply the first approach. Note, that the IC  $e^+e^-$  pair cascade considered in this work does not take into account the synchrotron losses of  $e^+e^-$  pairs and assumes that secondary  $e^+e^-$  pairs radiate locally secondary  $\gamma$ -rays, i.e. at their production site. The conditions for such type of cascade are determined in Bednarek (B97, see Sect. 2). For completeness and due to some different details of the scenario considered in this paper, we discuss below some

important conditions for IC  $e^+e^-$  pair cascades occurring in the radiation field of the massive star.

Leptons injected into the radiation of the massive star (primary electrons and secondary  $e^+e^-$  pairs from the cascade) are immersed in the stellar wind and/or in the plasma outflow along the jet. Therefore, efficiency of the IC process is determined by the relative importance of the IC cooling time scale in respect to the characteristic escape time scale, determined by the advection time scale of  $e^+e^-$  pairs with the stellar and/or jet outflows. The IC cooling time of leptons, the Thomson regime, in the radiation of the massive star can be estimated from,

$$\tau_{IC} = m_e \gamma_e P_{IC}^{-1} \approx 4 \cdot 10^4 r^2 = (\gamma_e T_4^4) s; \quad (1)$$

where  $m_e$  and  $\gamma_e$  are the rest mass and the Lorentz factor of leptons,  $P_{IC}^{-1} = (4/3)c \tau_e^{-2}$  is the energy loss rate on IC of leptons,  $c$  is the velocity of light,  $\tau_e$  is the Thomson cross section,  $U_{rad} = \sigma_B T_s^4 r^2$ ,  $\sigma_B$  is the Stefan-Boltzmann constant,  $T_s = 10^4 T_4$  K and  $R = rr_?$  are the surface temperature of the massive star and the distance from the center of the massive star (in units of its radius). The characteristic escape time scale of leptons from their creation (acceleration) place, identified with their advection time scale with the jet or the wind plasma outflow, is

$$\tau_{esc} = R/v \approx 33 r_{?;12} r = v s; \quad (2)$$

where  $v = V/c$  is the velocity of the jet (or the stellar wind). It is assumed that typical radii of the massive stars are of the order of  $r_? = 10^{12} r_{?;12}$  cm. By comparing Eq. 1 and Eq. 2, we estimate the minimum Lorentz factor of leptons above which they cool locally,

$$\gamma_e > \gamma_{min} \approx 1.2 \cdot 10^4 r v = (T_4^4 r_{?;12}): \quad (3)$$

For example, in the case of the massive star in LS 5039,  $T_4 = 3.9$ ,  $r_{?;12} = 1$ , and  $v = 0.5$ , leptons with the Lorentz factors above,  $\gamma_{min} \approx 25 r$ , cool locally before escaping from the binary system.

Leptons with Lorentz factors,  $\gamma_{min}$ , produce  $\gamma$ -ray photons with energies,

$$E \approx (4/3) \gamma_{min}^2 \cdot 10^3 r^2 v^2 = (T_4^7 r_{?;12}^2) \text{ MeV}; \quad (4)$$

where typical energies of photons coming from the massive stars are  $\approx 3k_B T_s \approx 2.6 \cdot 10^6 T_4$  MeV. We conclude that spectra of  $\gamma$ -ray photons produced in the cascade (assuming local cooling of leptons) are correct above energies given by Eq. 4. For the parameters of the massive stars in LS 5039 and LSI + 61° 303, escaping  $\gamma$ -ray spectra are correct above

$10^3$  MeV, provided that production of  $\gamma$ -rays occur inside the jet and within  $r \approx 30 r_?$  from the center of the massive star. For the stellar wind region, the limits on the low energy cut-offs in the cascade  $\gamma$ -ray spectra are about two orders of magnitude lower due to much lower stellar wind velocities in respect to the plasma velocity in the jet.

However, for the Lorentz factors above  $10^5$  scattering of soft photons occurs in the Klein-Nishina (KN) regime. We approximate the IC cooling time of leptons in the KN regime by,

$$\tau_{IC}^{KN} = m_e \gamma_e P_{IC}^{-1} (KN=T) \approx 8 \cdot 10^6 r^2 \gamma_e = T_4^2 s; \quad (5)$$

where  $\tau_{KN=T} = m_e c^2 = 2 \cdot 10^6 T_4$ . By comparing the escape time scale,  $\tau_{esc}$ , with the IC cooling time scale in the

KN regime  $\tau_{IC}^{KN}$ , we obtain the upper limit on the Lorentz factor of leptons which are able to cool locally

$$\gamma_e < \gamma_{max} \approx 4 \cdot 10^4 r_{?;12} T_4^2 = (rv): \quad (6)$$

Therefore, we conclude that leptons with energies  $\approx 10$  TeV should be able to cool locally within a few stellar radii from the surface of the massive stars in LS 5039 and LSI + 61° 303.

In the calculations shown below we assume that synchrotron energy losses of leptons can be neglected in respect to the IC losses. This is correct provided that the surface magnetic fields of the massive stars fulfill the condition,

$$B_s < 40 T_4^2 \text{ G}; \quad (7)$$

obtained from the comparison of the synchrotron and IC energy losses of leptons in the Thomson regime. The simple limit given by Eq. 7 is valid under assumption on the  $B/r^2$  magnetic field dependence on the distance from the stellar surface. It neglects the inner dipole part of the magnetic field in which  $B/r^3$ . Therefore, real upper bound on the surface magnetic field is a factor of 2-3 larger than given by Eq. 7. For the massive stars in LS 5039 and LSI + 61° 303, these upper bounds (Eq. 7) are  $\approx 620$  G and  $\approx 320$  G. In the Klein-Nishina regime, i.e. for  $\gamma_e \approx 10^5$ , the limit on the magnetic field is more restrictive due to the decrease of the cross section. It has been discussed in details by Bednarek (1997, see Fig. 4 in that paper).

Under conditions specified above (neglected synchrotron losses of leptons and their local isotropization), we study the features of the  $\gamma$ -ray spectra emerging from the binary system, due to the propagation effects in the radiation of their massive companions, assuming that primary particles, i.e. electrons or  $\gamma$ -rays, are isotropically injected somewhere along the jet. We consider the primary particles with the power law spectra and spectral index equal to 2 due to the equally distributed power per decade. The high energy cut-off in these primary spectra is assumed at 10 TeV (to be consistent with the observations of  $\gamma$ -ray spectrum from LS 5039 up to 4 TeV, Aharonian et al. (2005)). These initial spectra of particles are normalized to unity. The spectral index equal to 2 is also motivated by a relatively flat GeV  $\gamma$ -ray spectra observed from these two sources. The jets in microquasars move with much lower velocities (Doppler factor  $D \approx 1$ ) than these ones observed in active galactic nuclei. Therefore, the effects of relativistic beaming can be neglected in the first approximation.

#### 4.1 LS 5039

Let's at first consider the case of isotropic injection of primary electrons at the base of the jet, i.e.  $z = 0$ . In fact,  $\gamma$ -rays have to be injected at some distance from the accretion disk at which the disk radiation can be neglected in respect to the stellar radiation. The distance from the base of the jet at which the above condition can be fulfilled is estimated by comparing the energy density of the disk radiation with the energy density of the stellar radiation. These radiation fields are defined by the surface temperature of the massive star and the maximum temperature on the surface of the disk (at the disk inner radius,  $T_{in}$ ). We approximate the accretion disk radiation by the model of Shakura

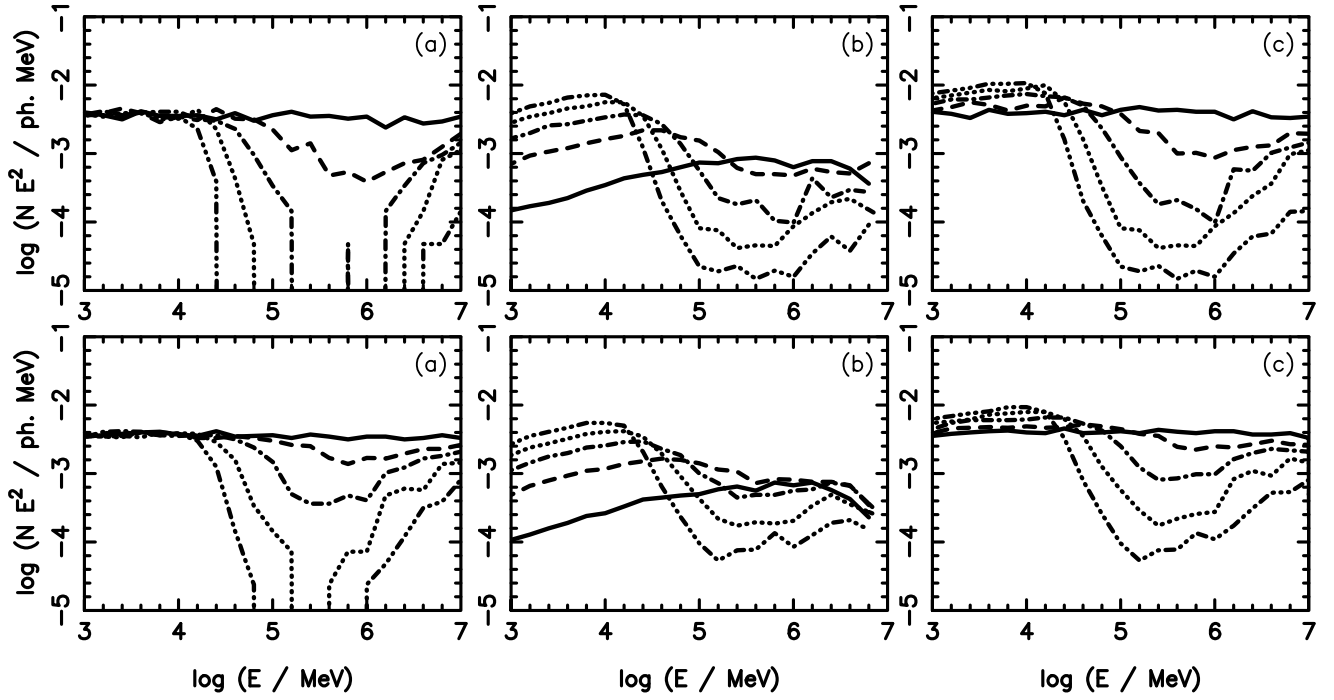


Figure 3. Differential  $\gamma$ -ray spectra (multiplied by the square of photon energy) escaping from the binary system at a specific range of the cosine angles  $\mu$ , measured in respect to the direction defined by the injection place and the center of the massive star. The range of  $\mu$  (with the width 0.1) are centered on 0.95 (full curve), 0.55 (dashed), 0.15 (dot-dashed), -0.25 (dotted), and -0.65 (dot-dot-dot-dashed).  $\gamma$ -rays are produced in the cascade initiated by primary  $\gamma$ -rays with the power law spectrum and spectral index 2 which are injected isotropically close to the base of the jet ( $z = 0$   $r_g$ , but sufficiently far away from the accretion disk), and at two distances from the massive star  $2.2r_g$  (upper figures, corresponding to the periastron passage of the compact object) and  $4.5r_g$  (bottom figures, corresponding to the apastron passage). (a) Spectra of primary  $\gamma$ -rays escaping without interaction. (b) Spectra of secondary  $\gamma$ -rays produced in the IC cascade. (c) Total spectra of  $\gamma$ -rays escaping from the binary system (the sum of spectra shown in (a) and (b)).

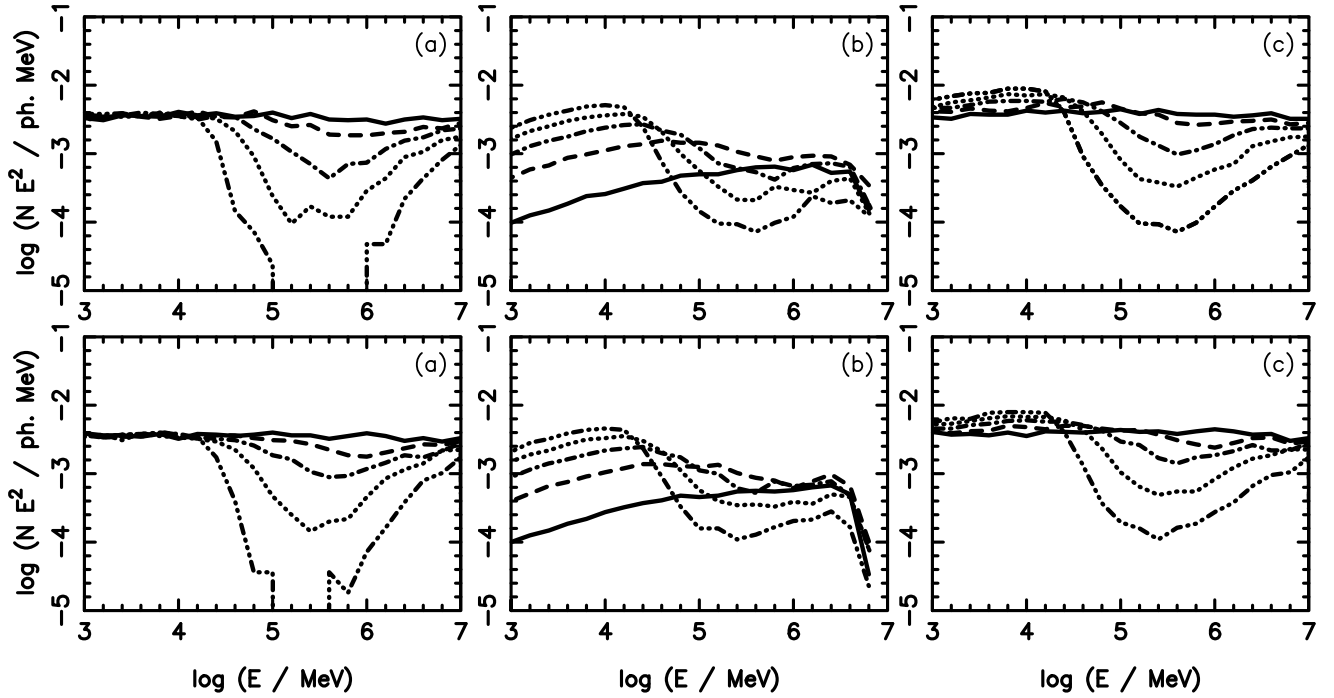


Figure 4. As in Fig. 3 but for the injection distance along the jet  $z = 5r_g$ . The distance of the injection place from the massive star is  $5.5r_g$  at the periastron (upper figures) and  $6.7r_g$  at the apastron (bottom figures).

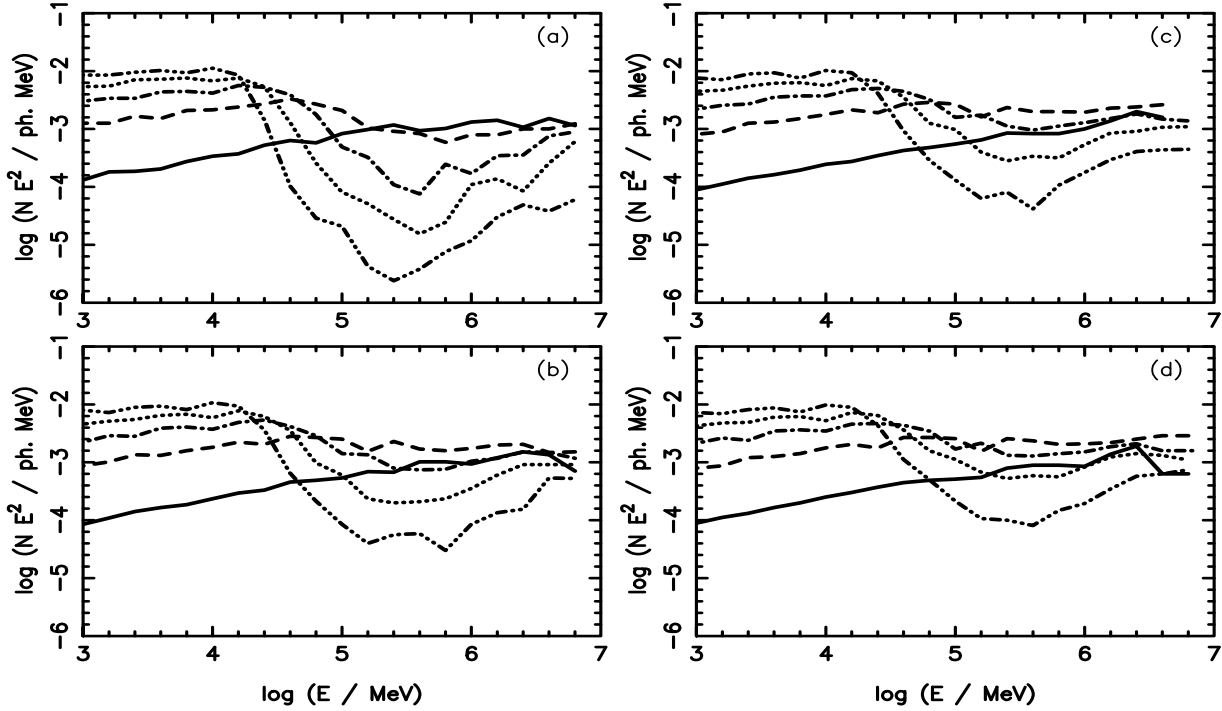


Figure 5. Total  $\gamma$ -ray spectra from the cascade initiated by isotropically injected primary leptons, with the power law spectrum and spectral index 2, at the range of cosine of the observation angles  $\cos \theta$ , with the width  $\Delta \cos \theta = 0.1$ . The spectra are shown for  $\cos \theta$  centered on 0.95 (full curve), 0.55 (dashed), 0.15 (dot-dashed), -0.25 (dotted), and -0.65 (dot-dot-dot-dashed), for two distances of the injection place from the massive star  $2.2r_g$  (figures (a) and (c)) and  $4.5r_g$  (figures (b) and (d)), corresponding to the periastron and the apastron of the injection place, respectively. The spectra are shown for the injection place at the base of the jet  $z = 0$   $r_g$  ((a) and (b)) and at the distance of  $z = 5r_g$  from the base of the jet ((c) and (d)).

& Sunyaev (1973) in which the disk radiation from its surface can be approximated by the black body radiation with some temperature gradient. The following condition has to be approximately fulfilled,

$$T_s^4 = r^2 T_{in}^4 (r_{in} = z)^2; \quad (8)$$

where  $r_{in}$  is the disk inner radius. From this condition, we estimate that above,

$$z = r_{in} r (T_{in} = T_s)^2; \quad (9)$$

the massive star radiation dominates over the accretion disk radiation. For typical parameters of the considered binary systems,  $T_s = 3 \cdot 10^4$  K,  $r = 10$ , the accretion disk inner radius  $r_{in} = 10^7$  cm, and  $T_{in} = 10^6$  K (limited by the condition that the disk thermal luminosity has to be lower than the observed X-ray luminosity from these binary systems,  $< 10^{35}$  erg s $^{-1}$ ), we estimate that above  $z = 10^7$  cm ( $> 0.1r_g$ ) from the base of the jet, stellar radiation dominates over accretion disk radiation. This condition is valid in the Thomson regime. However for the IC scattering process occurring in the Klein-Nishina regime, stellar radiation starts to dominate even at lower distances from the inner part of the disk, due to significantly larger temperature in the inner disk than on the stellar surface. These same arguments concern also possible disk corona which energy density can be comparable to the energy density of radiation from the surface of the disk but the characteristic temperature (average photon energies) are larger. The conditions for absorption of  $\gamma$ -ray photons in the radiation of the massive star are more favorable in respect to the radiation of

the accretion disk due to larger angular extend of the stellar disk in respect to the inner part of the accretion disk. In conclusion, we consider the injection of the primary  $\gamma$ -rays and electrons at the base of the jet assuming that it occurs at the distance,  $z > 0.1r_g = 0$ , which is very close to the base of the jet in respect to dimensions of the massive star.

Although primary  $\gamma$ -rays and soft photons from the massive star are injected isotropically, their injection places are located at different parts of the binary system (the jet or the compact object for primary  $\gamma$ -rays and the massive star for soft photons). Therefore, in fact primary  $\gamma$ -rays develop an IC  $e^+e^-$  pair cascade in the non-isotropic radiation field. The spectra, which emerge from the binary system, depend on the location of the observer in respect to direction defined by the location of the injection place and the center of the massive star (the angle measured from the outward direction defined by the injection place and the center of the massive star). We calculate the angle dependent spectra of  $\gamma$ -rays escaping from the binary system, by applying the Monte Carlo method (details are described in Bednarek 2000). Such method allows us to include the re-distribution of directions of secondary cascade  $\gamma$ -rays in respect to directions of their parent primary  $\gamma$ -rays, which is due to the isotropization of secondary cascade  $e^+e^-$  pairs and their preferable head on interactions with soft photons arriving from specific direction on the sky (i.e. inside the stellar disk limb). The parameters of  $\gamma$ -ray photons produced in the cascade (their energies and the escape angles) are sorted at a specific range of the cosine angles,  $\cos \theta$ , with the width of  $\Delta \cos \theta = 0.1$ .

We show the spectra of primary  $\gamma$ -rays which escape from the radiation field of the massive star without absorption (Fig. 3a), the spectra of  $\gamma$ -rays produced as a secondary cascade products (Fig. 3b), and the sum of these two, i.e. the total  $\gamma$ -rays spectra (Fig. 3c), for primary  $\gamma$ -rays injected at the distance  $z = 0$  along the jet, and for two locations of the compact object on its orbit, at the periastron distance from the massive star ( $2.2r_*$ , upper figures in Fig. 3) and at the apastron distance ( $4.5r_*$ , bottom figures). Simple absorption effects of primary  $\gamma$ -rays, for both distances of the injection place from the massive star, are very strong (see Fig. 3a). Primary  $\gamma$ -rays with energies in the range between a few tens of GeV up to a few TeV are completely absorbed (the exact range depends strongly on the observation angles), provided that the observation angles lay within the hemisphere containing the massive star. However, these strong deficits of  $\gamma$ -rays (between  $0.1 - 1$  TeV) are partially filled by the secondary cascade  $\gamma$ -rays (see Fig. 3b). The secondary  $\gamma$ -rays contribute also to the total  $\gamma$ -ray spectrum below  $\sim 10$  GeV escaping in the outward directions, i.e. for  $\theta > 90^\circ$  (Fig. 3b). Total  $\gamma$ -ray spectra (Fig. 3c) strongly depend on the observation angle. They show strong deficit above  $\sim 100$  GeV (a dip up to two orders of magnitudes) and the excess (up to a factor of two) in respect to the shape of the primary power law spectrum for large angles. However, they become more similar to the injected  $\gamma$ -ray spectrum for small  $\theta$ . As expected,  $\gamma$ -ray spectra escaping from the binary system for the injection places located at larger distances from the massive star (at the apastron passage), are less modified by the cascading processes than these ones produced at the periastron passage. The secondary  $\gamma$ -ray spectra produced by primary  $\gamma$ -rays injected at the apastron passage show decline above a few TeV (Fig. 3b). This is due to the high energy cut-off in the spectrum of primary particles at 10 TeV and due to the average larger interaction angles between primary  $\gamma$ -rays and soft photons from the massive star at the apastron passage.

In Fig. 4 we also show the  $\gamma$ -ray spectra produced in the cascade for the periastron and the apastron distances assuming that the injection place is located at the distance of  $z = 5r_*$  from the base of the jet in order to have impression how significant are the  $\gamma$ -ray spectra on the production site in the jet. General features of these  $\gamma$ -ray spectra are quite similar to the case of injection at the base of the jet ( $z = 0$ ). Therefore, if the injection of primary  $\gamma$ -rays occurs with similar acceleration efficiency and spectrum along the jet within a few stellar radii from the base of the jet, then the angular distribution of  $\gamma$ -rays (and their spectra) formed in the cascade process show quite similar features in relation to the direction defined by the injection place and the massive star. Note however, that the  $\gamma$ -ray spectra toward the observer located at fixed direction in respect to the plane of the binary may look very different for these two injection places as we discuss in Sect. 5.

As a second scenario we consider the injection of primary electrons in the specific region of the jet. As above, we consider two locations for the injection place along the jet: the base of the jet (Fig. 5a,b) and the distance  $z = 5r_*$  from the base of the jet (Fig. 5c,d). The case of isotropic injection of primary electrons with the power law spectrum differs from previously considered case of isotropic injection of primary  $\gamma$ -rays since electrons have tendency of more frequent

production of the first generation of cascade  $\gamma$ -rays in the direction toward the massive star (the effect of non-isotropic radiation and kinematics of IC process). Therefore,  $\gamma$ -ray spectra which escape from the binary system in this second scenario resemble the secondary cascade  $\gamma$ -ray spectra produced in the case of injection of primary  $\gamma$ -rays (compare Figs. 3b and 4b with Fig. 5). Escaping  $\gamma$ -ray spectra strongly depend on the viewing angle not only in TeV range ( $> 100$  GeV) but also in the GeV range (see Fig. 5). Moreover, the  $\gamma$ -ray fluxes expected in these two energy ranges are strongly anticorrelated (large TeV flux is accompanied by low GeV flux and the opposite). This is due to the fact that at directions of the large optical depths the energy converted from primary electrons in the IC process to the TeV  $\gamma$ -rays is re-distributed to the GeV energies. In directions where the optical depths are low, the energy of TeV  $\gamma$ -rays is not so efficiently degraded in the cascade process to lower energies. As a result, relatively large TeV fluxes are accompanied by small GeV fluxes.

#### 4.2 LSI + 61° 303

The binary system LSI + 61° 303 differs in some aspects from LS 5039. Although both binaries contain massive stars with similar radii, the surface temperature of the star in LSI + 61° 303 is a factor of  $\sim 0.7$  lower which results in the radiation energy density by a factor of  $\sim 4$  lower. Also the distance of the compact object from the massive star in LSI + 61° 303 change in larger range, from  $1.5r_*$  up to  $9.15r_*$ . Therefore, primary  $\gamma$ -rays injected in the jet propagate through the radiation field which vary with larger amplitude with full orbital period than in LS 5039.  $\gamma$ -ray spectra escaping toward the observer for the case of injection of primary  $\gamma$ -rays and electrons change more significantly with the observation angle. As an example, we show the  $\gamma$ -ray spectra for the case of injection of primary  $\gamma$ -rays at the base of the jet, i.e. for  $z = 0$ , (Fig. 6), and at the distance  $z = 3r_*$  from the base of the jet (Fig. 7).  $\gamma$ -ray spectra for the periastron passage of the injection place are quite similar to these ones expected from LS 5039 (compare the results in the upper Figs. 3c and 4c with the upper Figs. 6c and 7c). The effects of the lower surface temperature of the massive star in LSI + 61° 303 and the distance at the periastron passage almost compensate. However, at the apastron passage and at the base of the jet, the absorption dips (above  $\sim 100$  GeV) are much lower in the case of LSI + 61° 303 (compare the bottom Figs. 6c and 7c with the bottom Figs. 3c and 4c). Even at the apastron passage of the compact object in LSI + 61° 303 and at the distance of injection place from the base of the jet  $z = 3r_*$ ,  $\gamma$ -ray spectrum above  $\sim 100$  GeV should still vary by a factor of  $\sim 5$  with the angle (see Fig. 7c). Note that secondary cascade  $\gamma$ -ray spectra produced by primary  $\gamma$ -rays, which are injected at large distance from the massive star (at the apastron passage and at  $z = 3r_*$ ), show strong cut-offs after  $\sim 2$  TeV. This is the result of a relatively weak absorption of primary  $\gamma$ -rays with energies above a few TeV, combined with the kinematics of the IC scattering process for the case of strongly anisotropic radiation field of soft photons from the massive star.

$\gamma$ -ray spectra emerging from the binary system LSI + 61° 303 in the case of injection of primary electrons at the periastron distance are very similar to the spectra expected



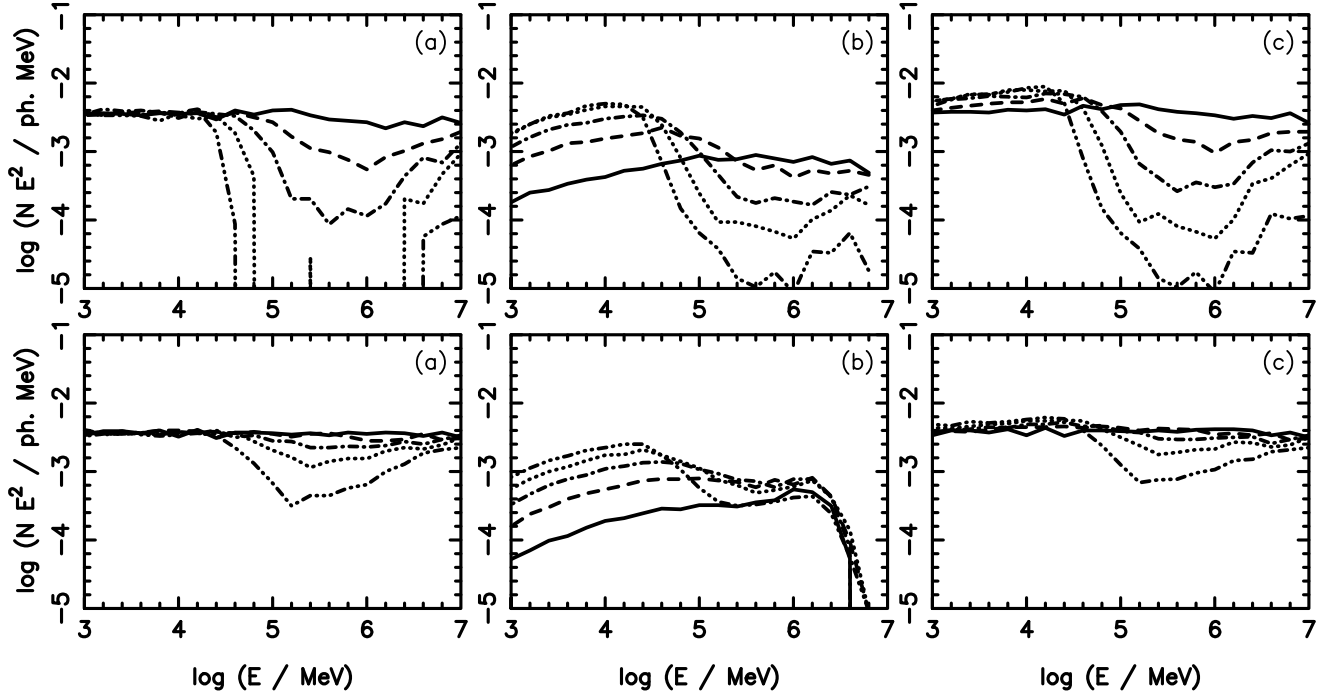


Figure 6. Differential  $\gamma$ -ray spectra escaping from the binary system at a specific range of the cosine angle (as in Fig. 3) but for the binary system LSI + 61° 303. The injection place of primary  $\gamma$ -rays is at the distance of the periastron passage ( $R = 1.5r_T$ , upper figures) and the apastron passage ( $9.15r_T$ , bottom figures) close to the base of the jet ( $z = 0$ ). The primary  $\gamma$ -rays spectra which escape without absorption are in (a), secondary cascade  $\gamma$ -ray spectra in (b), and the sum of (a) and (b), total escaping  $\gamma$ -ray spectra are in (c).

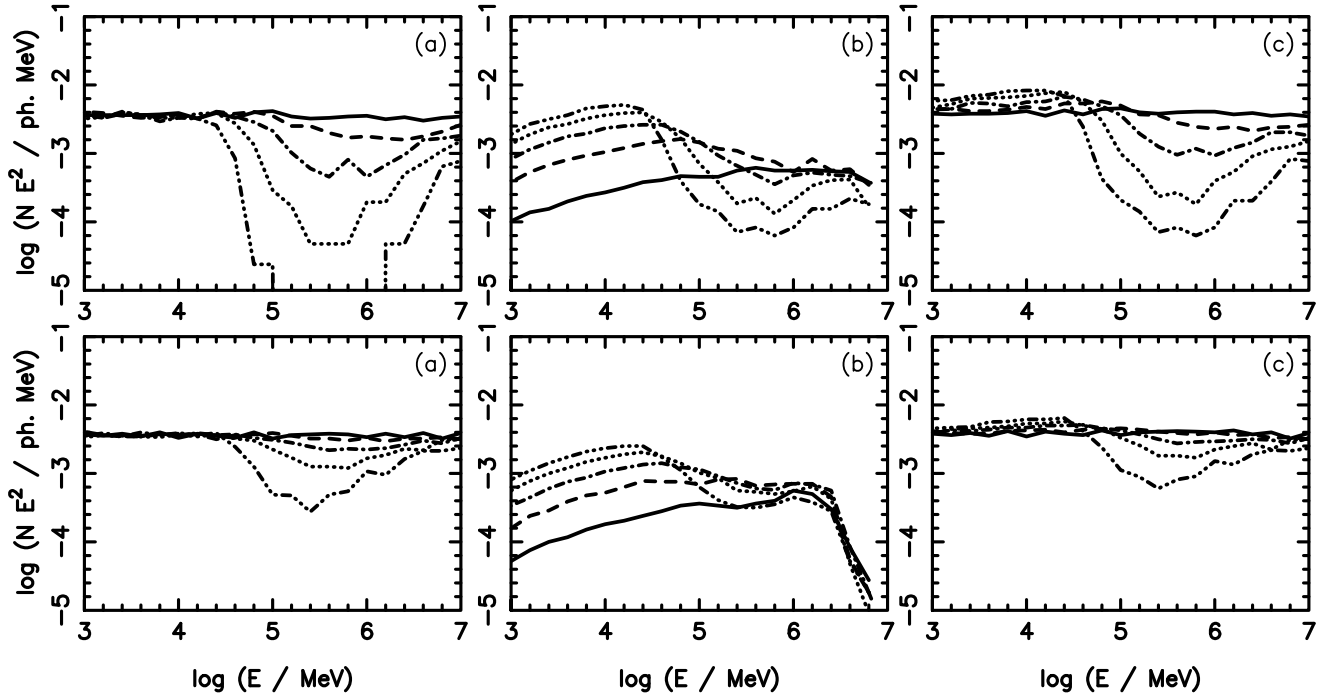


Figure 7. The  $\gamma$ -ray spectra produced by primary  $\gamma$ -rays (as in Fig. 6) but for the injection place of primary  $\gamma$ -rays and the distance  $z = 3r_T$  from the base of the jet. The distance of the injection place from the massive star is  $3.35r_{\text{star}}$  at the periastron (upper figures) and  $9.6r_T$  at the apastron (bottom figures).

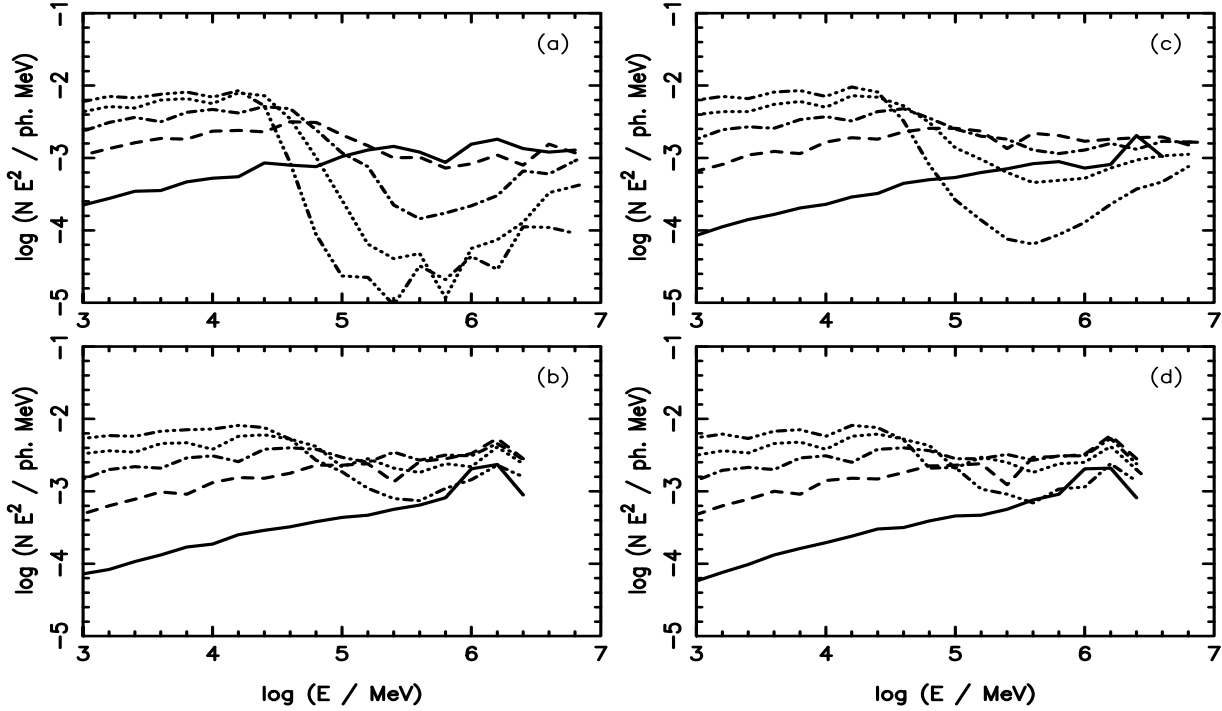


Figure 8. As in Fig. 5 but for LSI+61°303.  $\gamma$ -ray spectra are calculated for the injection place of primary electrons at the periastron distance (i.e. at  $1.5r_2$  – figures (a) and (c)) and at the apastron distance (i.e. at  $9.15r_2$  – figures (b) and (d)), and at the distance from the base of the jet  $z = 0$  (figures (a) and (b)), and  $z = 3r_2$  (figures (c) and (d)).

from LS 5039 (Fig. 5a,c with Fig. 8a,c). The absorption features are only slightly stronger.  $\gamma$ -ray spectra, produced by electrons injected farther from the base of the jet, e.g. at the distance  $z = 3r_2$ , are still strongly influenced by the cascade effects showing strong dependence on the observation angle in the GeV and TeV energy ranges (see Fig. 8c). However, at the apastron distance, the  $\gamma$ -ray spectra look different. They show strong dependence on the observation angle in the GeV energy range but relatively weak dependence in TeV energy range (e.g. Fig. 8b).  $\gamma$ -ray spectra produced at the apastron passage, but at distances from the base of the jet of the order of a few stellar radii, do not depend strongly on  $z$  (see Figs. 8b and d), since electrons injected at such distance still propagate in quite similar radiation field. In fact, for the apastron passage of the compact object in LSI+61°303 (at  $9.15r_2$ ), the distance of the injection place along the jet ( $z = 3r_2$ ) is located only at the distance of  $9.63r_2$  from the massive star (i.e. very similar to the apastron distance). Therefore, TeV  $\gamma$ -ray fluxes observed from LSI+61°303 at the apastron passage should be relatively larger in respect to their GeV fluxes in comparison to the expectations from the massive binary LS 5039 in which the TeV fluxes should be significantly lower than their corresponding GeV fluxes.

## 5 PHASE DEPENDENT GAMMA-RAY SPECTRA AND LIGHT CURVES

The observer is located differently in respect to the orbital plane of the binary systems LS 5039 and LSI+61°303. The inclination angles of the binary systems are probably quite similar, i.e. 25° in the case of LS 5039 (assuming that the

compact object is a black hole) and 30° applied in the case of LSI+61°303. However the azimuthal angles of the observer, measured in respect to the periastron passage, are 225° in LS 5039 and 70° in LSI+61°303. Therefore, phase dependent  $\gamma$ -ray spectra and  $\gamma$ -ray light curves expected from these two binary systems should have different features. Below we show the  $\gamma$ -ray light curves from these binaries at the GeV energies (1–10 GeV) and the TeV energies (>100 GeV), based on the calculations of the IC  $e^+e^-$  pair cascades occurring inside the radiation field of their massive stars. The phase dependent spectral features of the  $\gamma$ -ray emission are also discussed.

### 5.1 LS 5039

We have calculated the  $\gamma$ -ray luminosities escaping toward the observer as a function of the phase of the injection place of primary particles in the jet launched from the compact object in LS 5039. The light curves are obtained for two energy ranges, the GeV range (1–10 GeV) and the TeV range (>100 GeV), in the case of isotropic injection of primary  $\gamma$ -rays (Fig. 9a and c) and primary electrons (Fig. 9b and d), with the power law spectra and spectral index 2 (as discussed in Sect. 4.1). We consider the injection regions at the base of the jet,  $z = 0$  (full curves) and at the distance  $z = 5r_2$  (dashed curves) along the jet and two inclination angles of the observer  $\theta = 25^\circ$  (Fig. 9a and b) and  $\theta = 60^\circ$  (Fig. 9c and d). In order not to complicate the geometry too much, only the case of perpendicular propagation of the jet in respect to the plane of the binary system is considered. The calculations of the  $\gamma$ -ray spectra for the jets aligned at

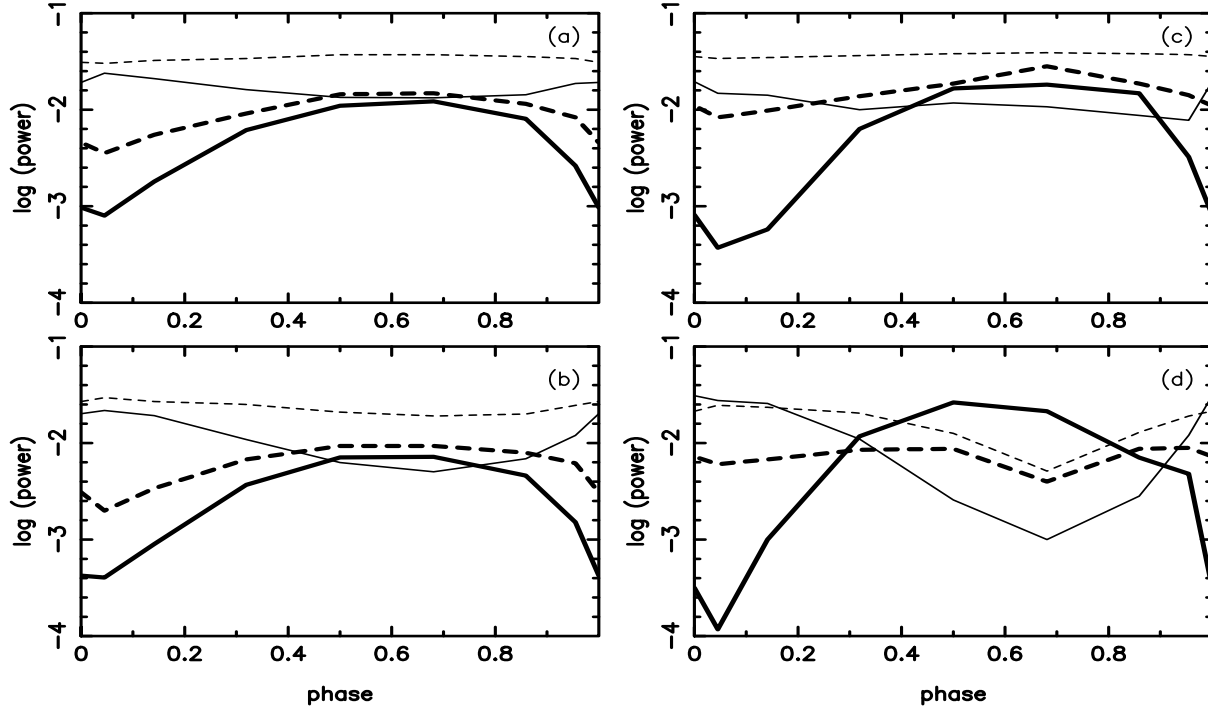


Figure 9. The power in  $\gamma$ -rays which escape from the binary system LS 5039 toward the observer (the  $\gamma$ -ray light curve) at the inclination angle  $\theta = 25^\circ$  ((a) and (b)) and  $\theta = 60^\circ$  ((c) and (d)), for the case of isotropic injection of primary  $\gamma$ -rays ((a) and (c)) and primary electrons ((b) and (d)), as a function of the phase of the injection place of the primary particles (phase is the time measured from the periastron passage divided by the orbital period of the binary system) at photon energies in the range 1-10 GeV (thin curves) and above 100 GeV (thick curves). The injection place of primary particles occurs in the jet. The light curves are shown for the injection place at the base of the jet  $z = 0$  (full curves) and at the distance  $5r_j$  along the jet (dashed curve).

some angle to the plane of the binary system are straightforward. They will be discussed in another work.

If the primary particles are injected at the base of the jet, then the  $\gamma$ -ray power in the GeV energy range vary by a factor of 2 and in TeV energy range by a factor greater than 10 for  $\theta = 25^\circ$  (see Fig. 9a and b). The maximum in TeV  $\gamma$ -ray light curve occurs at the phase 0.6 and corresponds to them in minimum in the GeV  $\gamma$ -ray light curve. Therefore, based on these cascade calculations we predict clear anticorrelation between the GeV and TeV  $\gamma$ -ray fluxes. The level of variability of the GeV fluxes is larger in the case of injection of primary electrons in comparison to the injection of primary  $\gamma$ -rays since the primary (unabsorbed)  $\gamma$ -rays also contribute to the predicted total  $\gamma$ -ray light curve. Therefore, GeV  $\gamma$ -ray light curve is quite smooth for the case of injection of primary  $\gamma$ -rays. This feature might give some insight into the production mechanism of primary particles ( $\gamma$ -rays or electrons) allowing to distinguish which particles are accelerated, hadrons (responsible for the primary  $\gamma$ -rays) or electrons?. If primary particles are injected farther from the base of the jet, then the amplitude of the  $\gamma$ -ray emission drops in both energy ranges (see dashed curves in Fig. 9a and b). However, the level of variability is still larger in the case of injection of primary electrons.

The  $\gamma$ -ray light curves for the observer located at larger inclination angle, i.e.  $\theta = 60^\circ$ , show significantly larger variability than for  $\theta = 25^\circ$ . For example, the  $\gamma$ -ray power can change by almost an order of magnitude in the GeV energy range and by two orders of magnitudes in the TeV en-

ergy range for the case of injection of primary electrons (see Fig. 9d). Therefore, in principle the level of  $\gamma$ -ray variability might help to distinguish between different interpretations of the observational data concerning the inclination of the binary system in LS 5039 and put some insight on the nature of the compact object.

In Fig. 10 and 11, we show the  $\gamma$ -ray spectra which escape to the observer for a few selected phases (time from the periastron divided by the orbital period) of the compact object in all considered above scenarios for the case of the inclination of the binary system equal to  $\theta = 25^\circ$  and  $60^\circ$ , respectively. The cascade  $\gamma$ -ray spectra produced by primary particles injected at the base of the jet drop suddenly above a few tens of GeV, reach their minimum at a few 100 GeV and become flat (spectral index  $< 2$ ) at higher energies. Between 0.1 - 1 TeV, the spectral index does not change significantly with the phase of the injection place. The TeV  $\gamma$ -ray deficit is larger for the injection of primary electrons and for larger inclination angles. However, the spectral indexes in the GeV and TeV energies are close to two in spite of such large difference in the level of emission. These features are generally consistent with the observations of LS 5039 in the GeV and TeV energy ranges. The spectra look completely different for the injection place farther along the jet. For example, already at the distance of  $5r_j$  from the base of the jet and  $\theta = 25^\circ$ , the total cascade  $\gamma$ -ray spectra are almost independent on the phase of the compact object in the case of injection of primary  $\gamma$ -rays (see Fig. 10b). However, for larger inclination angles of the binary, e.g.  $\theta = 60^\circ$ , small ab-

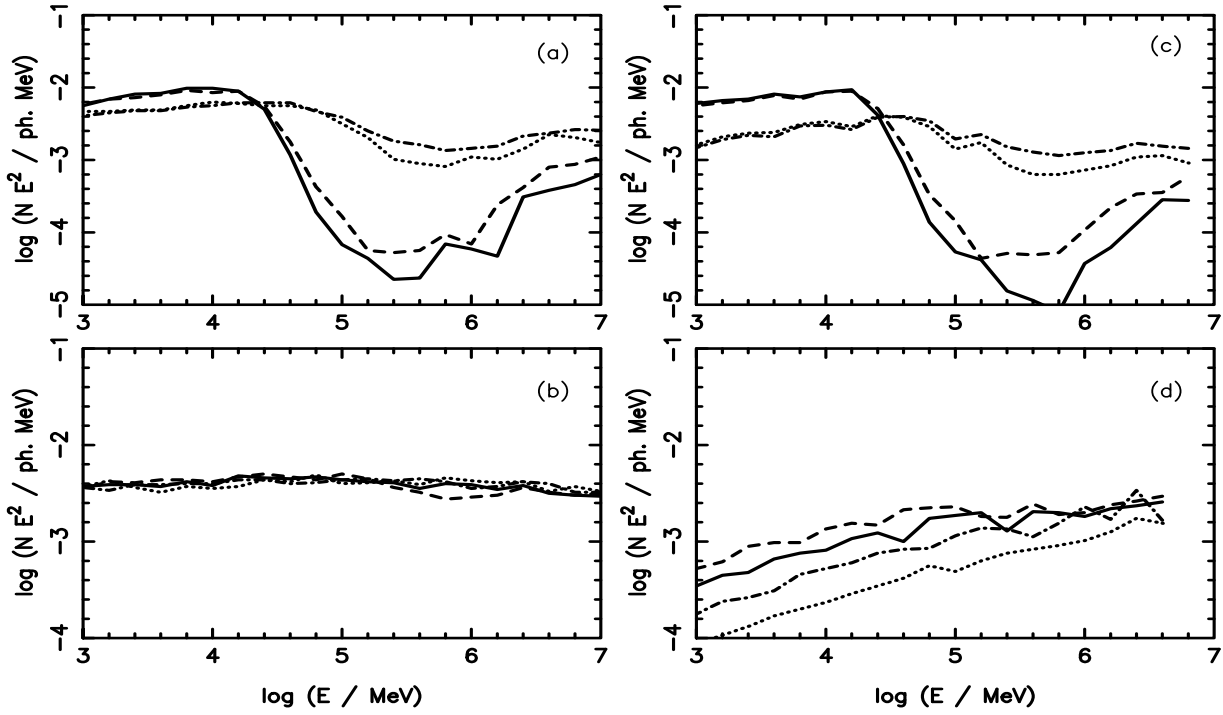


Figure 10.  $\gamma$ -ray spectra which escape from the binary system LS 5039 toward the observer at the inclination angle  $i = 25^\circ$  for different locations of the injection place of the source of primary particles ((a) and (b) –  $\gamma$ -rays, and (c) and (d) – electrons) defined by the azimuthal angle measured from the periastron:  $\phi = 0^\circ$  (full curve),  $90^\circ$  (dashed),  $180^\circ$  (dot-dashed), and  $270^\circ$  (dotted), and at the distance from the base of the jet  $z = 0r_j$  ((a) and (c)) and  $z = 5r_j$  (figures (b) and (d)).

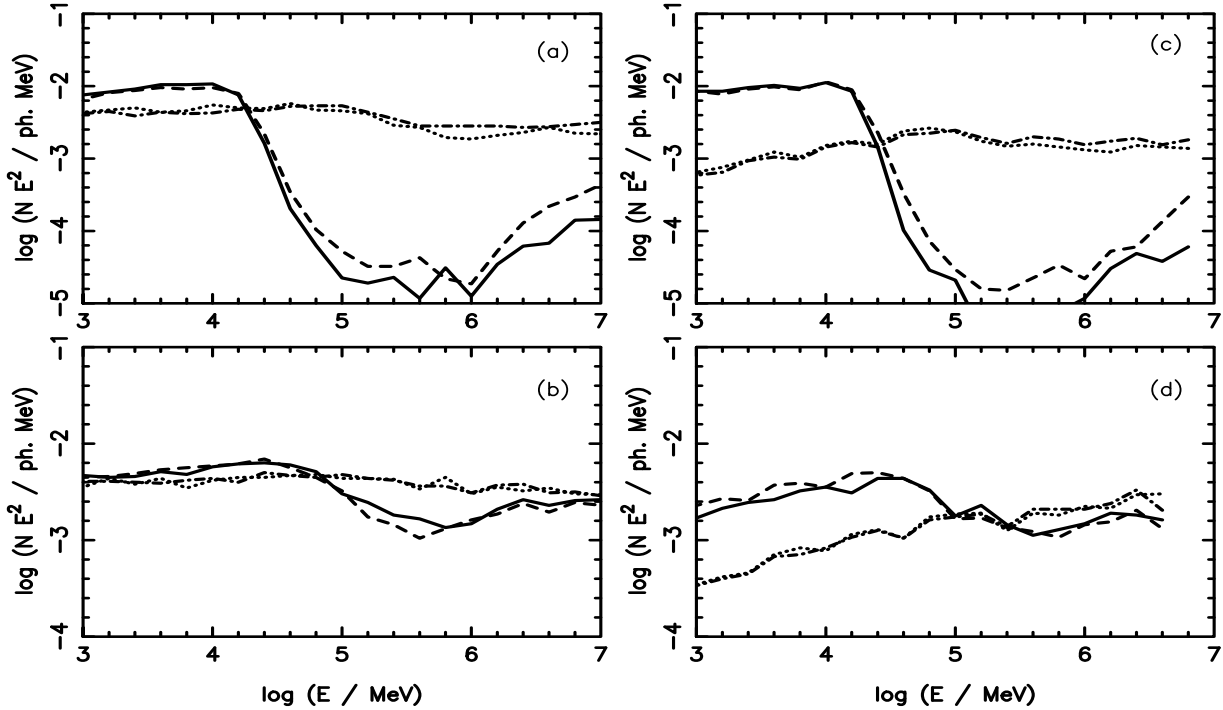


Figure 11. As in Fig. 10 but for the inclination angle of the binary system  $i = 60^\circ$ .

sorption feature starts to appear at TeV energies when the compact object is at the periastron. In the case of injection of primary electrons, the TeV  $\gamma$ -ray spectra are on similar level but differ significantly in the GeV energies. This GeV spectrum is flatter than in the case of injection of primary  $\gamma$ -rays (spectral index close to 1.5 versus a slightly flatter than 2), due to the lack of domination of the GeV spectrum by the primary  $\gamma$ -rays. These weak dependences of the  $\gamma$ -ray spectra in the TeV energies are due to small differences in the angles between the observer and the injection place of the primary particles farther from the base of the jet (e.g. considered here  $z = 5r_g$ ) for different phases of the binary system. Note however, that these angles show stronger differences for larger inclination angles of the binary system (compare Fig. 10 and Fig. 11).

## 5.2 LSI + 61° 303

The features of the  $\gamma$ -ray light curves and phase dependent spectra expected from the binary system LSI + 61° 303 are qualitatively similar to these ones discussed above for the binary system LS 5039 (see Figs. 12 and 13). However, there are also some significant differences. For example, the maximum in TeV  $\gamma$ -ray light curve of LSI + 61° 303 is broader and appears at the phase 0.2-0.5. The level of variability at TeV energies is smaller (variability by a factor less than 10). The anticorrelation between the GeV and the TeV fluxes is not so excellent as in LS 5039 (possible shift in phase by 0.2). Significantly smaller variability is expected in the GeV and TeV energy ranges, if the primary  $\gamma$ -rays are injected already at the distance of  $3r_g$  from the base of the jet. The level of variability in the GeV range is larger in respect to the TeV energy range when compared to the results obtained for LS 5039 in the case of the primary electrons injected at the distance of  $3r_g$  from the base of the jet. The absorption dips in the TeV  $\gamma$ -ray energy range are shallower than expected in LS 5039.

In summary, propagation effects influence in similar way the  $\gamma$ -ray spectra escaping from the binary system LSI + 61° 303 and LS 5039 when the injection place of the primary particles is relatively close to the massive stars (not far from the periastron passage and for small distances from the base of the jet). However, significant differences are expected for the injection of primary electrons farther along the jet and at the apastron passage as shown in Figs. 12 and 13.

## 6 CONCLUSIONS

We have performed Monte Carlo simulations of the propagation of high energy  $\gamma$ -rays inside compact massive binaries of the microquasar type, applying as an example parameters of LS 5039 (recently observed in TeV  $\gamma$ -rays and suggested as a counterpart of the EGRET source) and LSI + 61° 303 (similar parameters to LS 5039 and also suggested as a counterpart of the EGRET source). In both sources the optical depths for TeV  $\gamma$ -rays are greater than unity for most of the propagation directions, provided that the injection place of primary particles ( $\gamma$ -rays or electrons) is relatively close to the base of the jet launched from the inner part of the accretion disks around compact objects. Therefore, these primary

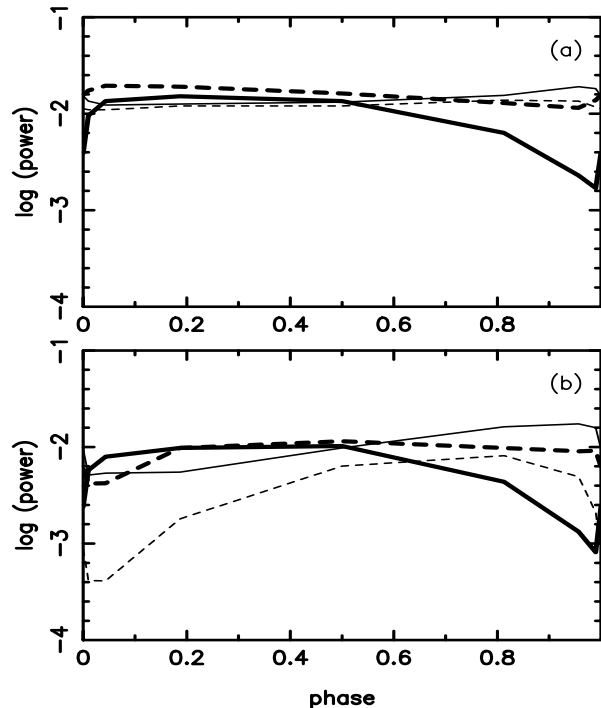


Figure 12. As in Fig. 9 but for the binary system LSI + 61° 303 ( $i =$  or the inclination  $= 30^\circ$ ). Primary  $\gamma$ -rays (figure a) and primary electrons (b) are injected at the distance from the base of the jet  $z = 0r_g$  (full curves) and  $z = 3r_g$  (dashed curves).

particles initiate IC  $e^+e^-$  pair cascades in the anisotropic radiation of the massive stars. We have calculated the  $\gamma$ -ray spectra produced in such cascades and investigated their basic features. It is concluded that the absorption dips in TeV  $\gamma$ -ray spectra emerging toward the observer are not so drastic as predicted in the earlier papers, e.g. by Bottcher & Demer (2005) and Dubus (2005). This is clearly seen by comparing  $\gamma$ -ray spectra calculated with pure absorption (e.g. Figs. 3a, 4a, 6a, and 7a) with the corresponding total  $\gamma$ -ray spectra produced in the cascade processes inside the binary system (Figs. 3c, 4c, 6c, and 7c). This less pronounced dips are due to the re-distribution of energy in the primary spectrum of  $\gamma$ -rays from the region above 1 TeV to 0.1–1 TeV energy range. Since the soft radiation field created by the massive stars in these two binaries are quite similar during periastron passages of their compact objects, the  $\gamma$ -ray spectra produced in the cascade processes do not differ significantly in the case of LS 5039 and LSI + 61° 303. However, the propagation effects are responsible for essential differences at the apastron passage, since LSI + 61° 303 is more extended (the apastron distance in LSI + 61° 303 is a factor of 2 larger than in LS 5039).

Let us concentrate at first on the features of  $\gamma$ -ray emission from LS 5039. The  $\gamma$ -ray luminosity from this source observed in the GeV energy range (assuming that the identification with the EGRET source by Paredes et al. 2000 is correct) is about two orders of magnitude larger than observed in TeV energy range (Aharonian et al. 2005b). However, spectra reported in these two energy ranges are quite similar (spectral index close to 2). These spectral features can be naturally explained by the propagation effects considered in this paper, i.e. IC  $e^+e^-$  pair cascading processes, inside

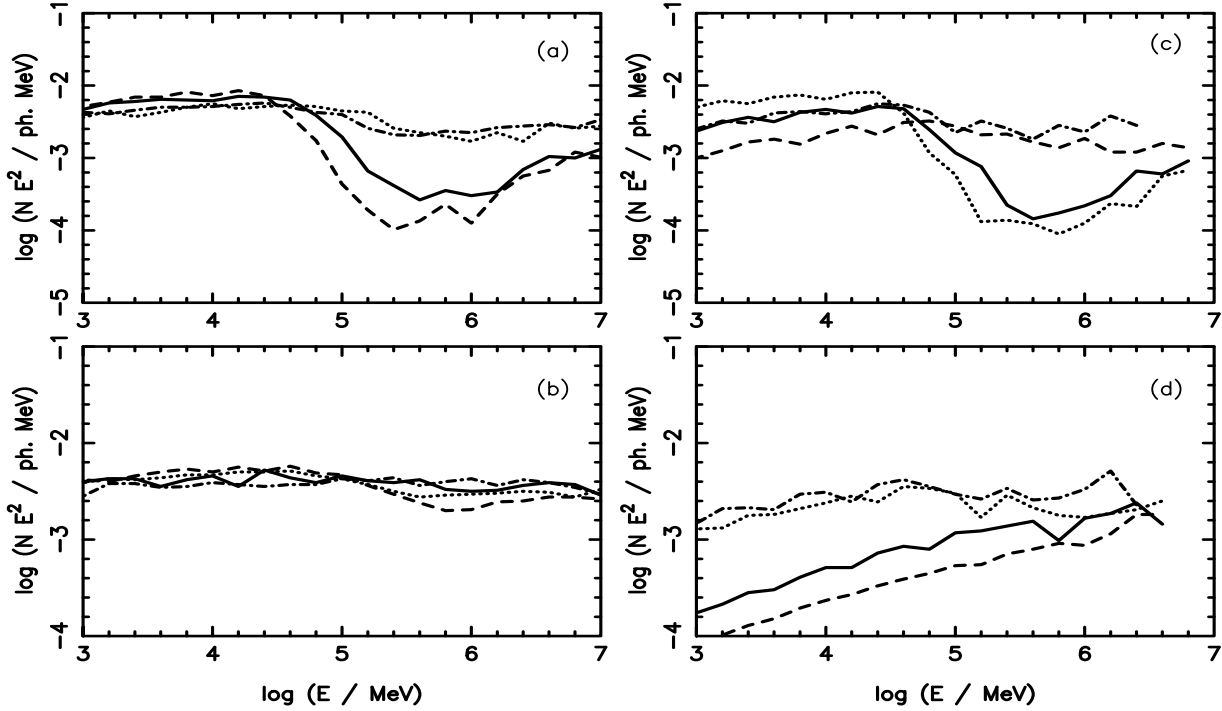


Figure 13. As in Fig. 10 but for LSI + 61° 303. Primary  $\gamma$ -rays (figures (a) and (b)) and primary electrons (figures (c) and (d)) are injected at the distance from the base of the jet  $z = 0 r_g$  (figures (a) and (c)) and  $z = 3 r_g$  (figures (b) and (d)).

the binary system. The primary  $\gamma$ -rays or electrons could be injected with a simple power law spectrum (and spectral index close to 2), relatively close to the base of the jet. The  $\gamma$ -ray luminosity expected in this propagation model at GeV energies ( $1 - 10$  GeV) should vary by a factor of  $\sim 2 - 3$ , and at TeV energies ( $> 100$  GeV) by a factor of  $\sim 10$  with the orbital period of the binary system LSI 5039. In fact, possible variation of the TeV signal by a factor of  $\sim 3$  has been recently suggested by Casares et al. (2005), although not statistically significant (Aharonian et al. 2005b). Moreover, we show that, due to the propagation (IC  $e^+e^-$  pair cascade) effects, the maximum in TeV  $\gamma$ -ray light curve should occur at phase  $\sim 0.6$  (measured as an azimuthal angle from the periastron passage, see Fig. 1). This seems to be inconsistent with the recent suggestion by Casares et al. (2005b) who, reanalyzed the HESS data with the new orbital parameters and, concluded that maximum of TeV emission occurs at the phase  $\sim 0.9$ . This discrepancy does not allow us to put any definite conclusions since the error bars in TeV  $\gamma$ -ray light curve, shown by Casares et al. (2005b), are very large. However, if real, it can give some information on the efficiency of acceleration process of the primary particles occurring in the jet (possibly linked with the efficiency of the accretion process) with the phase of the compact object on its orbit around the massive star.

Based on the propagation calculations it is concluded that  $\gamma$ -ray spectra produced in such IC  $e^+e^-$  pair cascades should show clear anticorrelation between the fluxes in the GeV and TeV energy ranges (see the light curves in Fig. 9). We also investigated the dependence of the propagation effects on the distance of the injection place from the base of the jet. If primary particles are injected already at the distance of a few stellar radii from the base of the jet (the case

of  $z = 5 r_g$  is discussed), then  $\gamma$ -ray fluxes expected from LSI 5039 do not vary strong enough to explain relative luminosities in the GeV and TeV energy ranges. Either a more complex shape for the spectrum of primary particles injected into the jet is required, e.g. composed of at least three different power laws, or two different populations of primary particles are needed, or the origin of different parts of  $\gamma$ -ray spectra in different regions of the jet has to be postulated. Moreover, the shape of the  $\gamma$ -ray spectra escaping toward the observer depends also on the inclination angle of the binary system which is not at present well known (estimated on  $25^\circ$  for the case of a solar mass black hole and on  $60^\circ$  for the case of a neutron star). The level of variability of the TeV emission for the injection place of primary particles at the base of the jet is clearly larger for the inclination angle  $\sim 60^\circ$  than for  $\sim 25^\circ$ . However these differences seem to be too low in order to put constraints on the inclination angle of binary system LSI 5039 based only on the observations with the present sensitivity Cherenkov telescopes.

If the identification of the binary system LSI + 61° 303 with the EGRET source 3EG J0241+ 6103 is correct (see introduction), then average  $\gamma$ -ray luminosity ( $> 100$  MeV),

$\sim 8 \cdot 10^4 \text{ erg s}^{-1}$ , is only about a factor of three lower than in the case of LSI 5039. This suggests that  $\gamma$ -ray properties of these two sources should be quite similar. Our simulations of the propagation of primary  $\gamma$ -rays show that absorption of  $\gamma$ -rays is similar in both binaries at the periastron passage of the compact object (if primary particles are injected at the base of the jet) but is less important at the apastron passage of LSI + 61° 303. The TeV fluxes from LSI + 61° 303 predicted by the propagation effects should be relatively larger in respect to its GeV fluxes than observed in the binary system LSI 5039. This feature might help in detection of LSI

+ 61° 303 at TeV energies. The maximum in TeV  $\gamma$ -ray light curve predicted by the propagation effects in LSI + 61° 303 should occur at the phase 0.2–0.4, measured from the periastron. The TeV  $\gamma$ -ray signal is expected to be modulated by an order of magnitude with the maximum for the case of injection of primary electrons injected farther along the jet (at a distance of a few stellar radii, see the case of  $z = 3r_2$  in Fig. 12). A also strong variability of the GeV flux is possible (even by an order of magnitude) for the case of injection of primary electrons farther from the base of the jet (see e.g. the case of  $z = 3r_2$  in Fig. 12b). Injection of electrons at the base of the jet predicts modulation by a factor of  $\sim 2$  with the minimum when the compact object is in front of the massive star. Re-analysis of the EGRET data indicates probable modulation of the GeV signal from the source toward LSI + 61° 303 (Tavani et al. 1998, Wallace et al. 2000) with the maximum emission near periastron (Massi 2004). This is inconsistent with the predictions of studied here propagation effects for the case of injection of primary electrons which show deficit of GeV emission close to periastron. Therefore, if this modulation is real then the mechanism responsible for such modulation of GeV emission should be even much more efficient since considered here propagation effects work in opposite direction. For the case of isotropic injection of primary  $\gamma$ -rays, the GeV signal is only weakly modulated with the period of the binary system due to the domination of primary  $\gamma$ -rays at such low energies.

In this paper we have only analyzed the effects of propagation of  $\gamma$ -rays inside these two binary systems assuming that efficiency of particle acceleration and spectra of injected particles do not depend on the location of the injection place of primary particles along the jet, i.e. they are uniformly distributed along the jet, i.e. from  $z = 0r_2$  to at  $z = 5r_2$  (LS 5039) or  $3r_2$  (LSI + 61° 303). Proper analysis of  $\gamma$ -ray emission from these sources require, except considering the IC  $e^+e^-$  pair cascade effects, a detailed model for efficiency of accretion process, conversion of accretion energy into particles, acceleration of particles (their spectra), and production of  $\gamma$ -rays. Such models, which unfortunately do not take into account the cascade effects analyzed in this paper but discuss only production of  $\gamma$ -rays in the Inverse Compton process far away from the base of the jet, have been recently discussed by Bosch-Ramón, Romero & Paredes (2005) and Demer & Bottcher (2005).

#### ACKNOWLEDGMENTS

I would like to thank the referee, Dr G. Dubus, for many useful comments. This work is supported by the Polish M N II grant No. 1P 03D 01028 and the KBN grant PBZ KBN 054/P 03/2001.

#### REFERENCES

- Aharonian, F., Akhperjanian, A. G., Aye, K. M., et al. 2005a A & A, 442, 1  
 Aharonian, F., Akhperjanian, A. G., Aye, K. M., et al. 2005b Science 309, 746  
 Atoyan, A. M. et al. 2002 A & A, 383, 864

- Bednarek, W., Giovannelli, F., Karakula, S., Tkaczyk, W. 1990 A & A, 236, 175  
 Bednarek, W. 1993 A & A, 278, 307  
 Bednarek, W. 1997 A & A 322, 523 (B 97)  
 Bednarek, W. 2000 A & A 362, 646 (B 00)  
 Bosch-Ramón, V., Paredes, J. M. 2004a A & A 417, 1075  
 Bosch-Ramón, V., Paredes, J. M. 2004b A & A 425, 1069  
 Bosch-Ramón, V., Romero, G. E., Paredes, J. M. 2005 A & A in press (astro-ph/0509086)  
 Bottcher, M., Demer, C. D. 2005 ApJ 634, 81  
 Carramiñana, A. 1992 A & A, 264, 127  
 Casares, J., Ribas, I., Paredes, J. M., Martí, J., Allende Prieto, C. 2005a MNRAS, 360, 1105  
 Casares, J., Ribas, I., Ribas, I., Paredes, J. M., Martí, J., Herrero, A. 2005b MNRAS, 364, 899  
 Chadwick, P. M., et al. 1998 ApJ, 503, 391  
 Chadwick, P. M., et al. 1999 ApJ, 513, 161  
 Demer, D. C., Bottcher, M. 2005, ApJ, submitted (astro-ph/0512162)  
 Dubus, G. 2005 A & A, submitted (astro-ph/0509633)  
 Gregory, P. C., Taylor, A. R. 1978 Nature 272, 704  
 Hall, T. A. et al. 2003 ApJ 583, 853  
 Hemsen, W., et al. 1977 Nature 269, 494  
 Knien, D. A. et al. 1997 ApJ 486, 126  
 Maraschi, L., Treves, A. 1981 MNRAS, 194, 1  
 Massi, M. 2004 A & A, 422, 267  
 Massi, M. et al. 2004 A & A, 414, L1  
 Mori, M. et al., 1997 ApJ, 476, 842  
 Moskalenko, I., Karakula, S., Tkaczyk, W. 1993 MNRAS, 260, 681  
 Paredes, J. M. Proc. 2<sup>nd</sup> Int. Sym. High Energy Gamma-Ray Astr., Eds. Aharonian F. et al., (Heidelberg – Germany), AIP v. 745, 93  
 Paredes, J. M., Martí, J., Ribas, I., Massi, M. 2000 Science 288, 2340  
 Paredes, J. M., Bosch-Ramón, V., Romero, G. E. 2005 A & A, in press (astro-ph/0509095)  
 Protheroe, R. J., Stanev, T. 1987 ApJ, 322, 838  
 Romero, G. E. 2004 Chin J Astron Astrophys., 5, 110  
 Romero, G. E., Christiansen, H. R., Orellana, M. 2005 ApJ, 632, 1093  
 Shakura, N. I., Sunyaev, R. A. 1973 A & A 24, 337  
 Sierpowska, A., Bednarek, W. 2005 MNRAS 356, 711 (SB 05)  
 Tavani, M., Knien, D., Mattox, J. P., Paredes, J. M., Foster, R. S. 1998 ApJ, 497, L89  
 Thompson, D. J. et al. 1995 ApJS, 101, 259  
 van Dijk, R. et al. 1996 A & A, 315, 485  
 Vestrand, W. T., Sreekumar, P., Mori, M. 1997 ApJ, 483, L49  
 Wallace, P. M. et al. 2000 ApJ, 540, 184  
 Weekes, T. C. 1988 PhysRep. 160, 1